RESEARCH ARTICLE | MAY 16 2023

Simulation study of a linear quadratic control for active seat suspension systems

Ali I. Al-Zughaibi ✉; Emad Q. Hussein; Noor A. Huseein

AIP Conference Proceedings 2631, 030005 (2023)
https://doi.org/10.1063/5.0131601

Simulation Study of a Linear Quadratic Control for Active Seat Suspension Systems

Ali I. Al-Zughaibi [a)], Emad Q. Hussein [b)], and Noor A. Huseein [c)]

College of Engineering, University of Kerbala, Kerbala, Iraq.

[a)] Corresponding author: ali.i@uokerbala.edu.iq
[b)] emad.dujaily@uokerbala.edu.iq
[c)] noor.a@s.uokerbala.edu.iq

Abstract. There is currently an increasing focus on enhancing driver's seat suspension systems to reduce the vibration transmitted to the human body from road conditions that can negatively affect driver performance, as well as potentially leading to health risks. An active seat suspension system with a closed-loop controller to generate an external force to reduce the vertical vibration transmitted to the seat pan is thus in development, and this paper represents an approach to designing an active seat suspension control system using the linear quadratic regulator control technique. A MATLAB environment was used to simulate the design, while analysis of the driver's seat was done on a test rig model with two degrees of freedom. The active seat suspension system performance, assessed through adapting the linear quadratic regulator approach, was considered to compare well with passive responses. By generating the optimal values for input control and state matrix in terms of affecting the control action, the simulation results show that the optimal active seat controller has good potential to reduce vertical acceleration by an approximate range of 90%, thus achieving the required ride comfort within the designated cost constraints.

1. INTRODUCTION

In recent years, both scientists and vehicle makers have focused their efforts on developing novel technologies for providing more comfortable and safer transport in heavy-duty vehicles. The most important parts of suspension design from this perspective are for it to be reliable and safe and to offer good performance in terms of nullifying road excitation [1]. A vehicle's suspension system often offers good performance in terms of reducing high-frequency vibrations caused by bumpy roads, yet many have poor isolative performance with respect to low-frequency vibrations, which has led to the more specific development of seat suspension systems to reduce the vibrations at low frequencies [2]. Vehicle drivers, especially truck drivers, are otherwise exposed to Whole-Body Vibrations (WBV), transferred to their bodies through the seats, which can affect both the drivers' health and efficiency. According to ISO 2631-1 1997, as WBV increases, ride comfort decreases, and health risks are also increased by increasing vertical acceleration. Thus, acceleration could be linked to comfort measurements [3][4].

A driver's seat suspension system aims to isolate the driver's body from the effects of road conditions and thus to maximise ride comfort. Driver seat suspension systems may be classified as passive, active, or semi-active suspension systems. In passive systems, insulation is achieved by using a spring with dampers and cushions. The springs support the seat's body, acting as an energy reservoir, while the damper is the dispersive energy element; however, this offers poor vibration isolation performance as compared with other types, particularly within the low frequencies range (1 to 10 Hz) [5]. Active systems, which do also incorporate passive elements, have a factor that supplies energy to the system, known as an actuator, with sensors to measure the force, motion, and acceleration that indicate a vibration signal. The actuator force is then primarily responsible for vibration isolation and cancellation procedures. Many types of actuators have been developed over the years, including hydraulic, pneumatic, electrohydraulic, electromagnetic, and stacked piezoelectric actuators [6][7]. The remaining suspension type, semi-active suspension, may be considered a melding of passive and active suspension systems to provide the best

5th International Conference on Engineering Sciences – ICES21
AIP Conf. Proc. 2631, 030005-1–030005-12; https://doi.org/10.1063/5.0131601
Published by AIP Publishing. 978-0-7354-4457-7/$30.00

performance possible. This is mainly achieved by adjusting passive elements using control strategies that require specific active devices, such as dampers, which may take the form of electrorheological and magnetorheological fluid dampers [8].

Several control strategies can be used to control active vibration systems, and some active seat suspension techniques have recently been developed to reduce vibrations and promote ride comfort. A Linear Quadratic Regulator (LQR) is now considered the best active control technique, having been adopted as a common form of optimal control strategy [9][10], being better than both PID and H∞ in terms of achieving ride comfort [11]. This study thus aimed to design an optimal LQR controller for a seat test rig as a way to enhance both ride comfort and road handling by reducing vertical acceleration. A comparison between passive and active systems was then done using a MATLAB environment.

2. MATHEMATICAL MODELING

The modelling for the active suspension seat system was based on an experimental passive seat test rig structure [12. The passive test rig consists of an input unit, which includes a lower part that contains an electric motor and cam to generate the input signal and an upper part, which supports the seat frame weight using four springs. The seat frame structure is a separate unit formed of a seat base that connects to the top part of the input unit and a seat pan that supports the driver's weight and which is connected to the base via a linear slider and two lever arms. The passive suspension element is a spring with a damper, which is connected to the seat base and to the seat pan via two vertical lever arms.

An active seat model with two degrees of freedom was used to model the test rig system. The seat test rig was thus modelled in the time domain using state-space to model LQR control. Figure 1 shows the active seat system model.

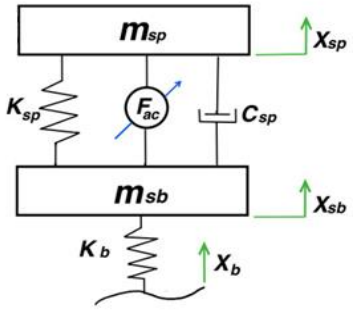

FIGURE 1. Active seat model.

A description of the model symbols is offered in Table 1.

TABLE 1: Active model symbols

Symbol	Description	Symbol	Description
m_{sp}	Seat pan mass + driver's mass (Kg)	F_a	Control force (N)
m_{sb}	Seat base mass (Kg)	X_{sb}	Vertical displacement of seat base (m)
k_{sb}	Seat base stuffiness (N\m)	X_{sp}	Vertical displacement of seat pan (m)
k_{sp}	Seat pan suspension stiffness (N\m)	X_b	Body excitation displacement (m)
c_{sp}	Seat pan suspension damper (N.s\m)		

The parameters used in this model are listed in Table 2.

TABLE 2: Parameters of the active seat suspension

Parameter	value
m_{sp}	58 Kg
k_{sp}	20000 N\m
c_{sp}	4000 N.s\m
m_{sb}	21 Kg
k_b	150000 N\m

The EOM in the vertical direction for the active system was derived through applying Newton's 2nd law of motion to the FBD as shown previously.

$$\ddot{x}_{sp} = \frac{1}{m_{sp}}\left[-c_{sp}\left(\dot{x}_{sp} - \dot{x}_{sb}\right) - k_{sp}\left(x_{sp} - x_{sb}\right) + F_a\right] \quad (1)$$

$$\ddot{x}_{sb} = \frac{1}{m_{sb}}\left[-k_b\left(x_{sb} - x_b\right) + c_{sp}\left(\dot{x}_{sp} - \dot{x}_{sb}\right) + k_{sp}\left(x_{sp} - x_{sb}\right) - F_a\right] \quad (2)$$

State variables were defined as

$$\boldsymbol{x_1 = x_{sp}} \ , \ \boldsymbol{x_2 = \dot{x}_{sp}} \ , \ \boldsymbol{x_3 = x_{sb}} \ , \ \boldsymbol{x_4 = \dot{x}_{sb}}$$

The state-space model thus represents the system dynamics in the form

$$\dot{x} = A_x + B_u$$
$$y = C_x + D_u \quad (3)$$

$$A = \begin{vmatrix}\dot{x}_1\\ \dot{x}_2\\ \dot{x}_3\\ \dot{x}_4\end{vmatrix}\begin{bmatrix} 0 & 1 & 0 & 0\\ \frac{-k_{sp}}{m_{sp}} & \frac{-c_{sp}}{m_{sp}} & \frac{k_{sp}}{m_{sp}} & \frac{c_{sp}}{m_{sp}}\\ 0 & 0 & 0 & 1\\ \frac{k_{sp}}{m_{sb}} & \frac{c_{sp}}{m_{sb}} & \frac{-k_{sb}-k_{sp}}{m_{sb}} & \frac{-c_{sp}}{m_{sb}}\end{bmatrix}\begin{vmatrix}x_1\\ x_2\\ x_3\\ x_4\end{vmatrix} \qquad B = \begin{vmatrix}\dot{x}_1\\ \dot{x}_2\\ \dot{x}_3\\ \dot{x}_4\end{vmatrix}\begin{bmatrix}0\\ 0\\ 0\\ \frac{k_{sb}}{m_{sb}}\end{bmatrix}\begin{vmatrix}F_a\\ x_b\end{vmatrix} \quad (4)$$

$$C = \begin{vmatrix}y_1\\ y_2\end{vmatrix}\begin{bmatrix}\frac{-k_{sp}}{m_{sp}} & \frac{-c_{sp}}{m_{sp}} & \frac{k_{sp}}{m_{sp}} & \frac{c_{sp}}{m_{sp}}\\ 1 & 0 & 0 & 0\end{bmatrix} \qquad D = \begin{vmatrix}y_1\\ y_2\end{vmatrix}\begin{bmatrix}1 & 0 & 0 & 0\\ 0 & 0 & 0 & 0\end{bmatrix}$$

where,

$x_b = input\ of\ system$ and $x_{sp}, \ddot{x}_{sp} = outputs\ of\ the\ system$

where A= state matrix, B= input matrix, C= output matrix, and D= disturbance matrix.

3. EXPERIMENTAL WORK

The driver test rig system was created and analysed in [12]. The experimental and simulation analysis results showed that the test rig offered good mechanical responses, with a reliable design that created good performance at low cost; this was thus confirmed as a source for developing a driver's vehicle seat. The seat pan displacement,

velocity, and acceleration results in particular showed a good agreement between simulation and experimental work on the full driver seat test rig.

The test rig showed room for performance improvement, however. This led to the proposal of a suitable LQR control system to check test rig performance. Two types of road profiles were then applied to the test rig model to compare the active and passive seat suspension.

4. LQR CONTROLLER DESIGN

The LQR control technique offers full state feedback control focused only on the constraints connected with system states. The idea of the LQR control technique is to minimise the energy associated with a given cost function to provide optimal control feedback gain to enhance closed loop stability and offer good system performance [13][14]. The cost function formula is

$$J_{LQR} = \int_0^\infty (x^T Q\, x + u^T R\, u)\, dt \tag{5}$$

Where

x is the state vector, and u is the control vector. Q (n×n) represents the weighting matrix of the system state [$Q=Q^T \geq 0$], while R (r×r) represents the weighting matrix of input control [$R=R^T \geq 0$].

The LQR state variable feedback is arranged as shown in fig. 2.

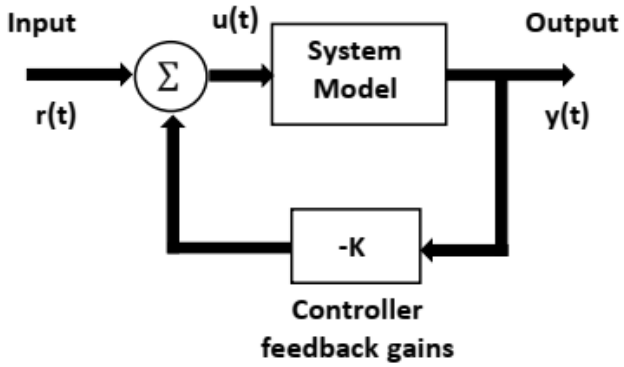

FIGURE 2. LQR feedback block diagram.

The Q and R matrixes must be carefully selected as they can help calculate the relative importance of existent system error and system energy dissipation [15]. The objective of the controller overall is to make the measured controlled output signal $y = Cx$ as small as possible.

The LQR control problem is frequently characterised by a more general description based on determining the control input to minimise a cost function:

$$J_{LQR} = \int_0^\infty (x^T * C^T \bar{Q}\, C * x + u^T * \rho\, \bar{R} * u)\, dt \tag{6}$$

Where

$$Q = C^T \bar{Q}\, C \quad \text{, and} \quad R = \rho\, \bar{R} \tag{7}$$

The $\boldsymbol{\rho}$ is a positive constant.

The term $\int_0^\infty (x^T * C^T \bar{Q}\, C * x$ represents the energy of the output, while the term $\int_0^\infty (u^T * \rho\, \bar{R} * u)\, dt$ represents the control signal energy.

In this paper, a version of Bryson's method is used to determine the initial weight matrixes $\bar{Q}$ & $\bar{R}$, with trial and error then used to accurately tune these two matrixes' parameters to achieve the best performance for the controller [16][17]. Bryson's method assumes that Q and R are diagonal matrixes, and thus only the weights Q_{ii} and R_{jj} are of

concern. This method suggests that the initial weight (diagonal elements) equals the reciprocal of the square of the value of maximum acceptable time-domain response set by the designer [18]. Bryson's method for $\bar{Q}$ matrix and $\bar{R}$ matrixes can thus be written as:

$$\bar{Q}_{ii} = \frac{1}{Max.[x_i]^2} \qquad \bar{R}_{jj} = \frac{1}{Max.[u_j]^2} \tag{8}$$

After calculating the Q and R matrixes, these can be used to find the value of P by substitution into the algebraic Riccati Equation [19]:

$$PA + A^T P + Q - PBR^{-1}B^T P = 0 \tag{9}$$

The P-value is then used to obtain K (feedback gain matrix) using the equation below:

$$u = -Kx \; = \; -R^{-1}B^T Px \tag{10}$$

A MATLAB environment was used to solve these equations and to calculate the K and P values in this work.

5. SIMULATION RESULTS AND DISCUSSION

The design goals are to achieve ride comfort in relation to acceleration and improved road handling in terms of road-holding related to suspension. These quantities should thus be minimised by the suggested LQR controller. The MATLAB/Simulink environments chosen for simulation were thus designed to check the performance of the LQR controller design; figure 3 shows the LQR control for the active seat test rig system, used with two different values for the Q matrix and five values for the R.

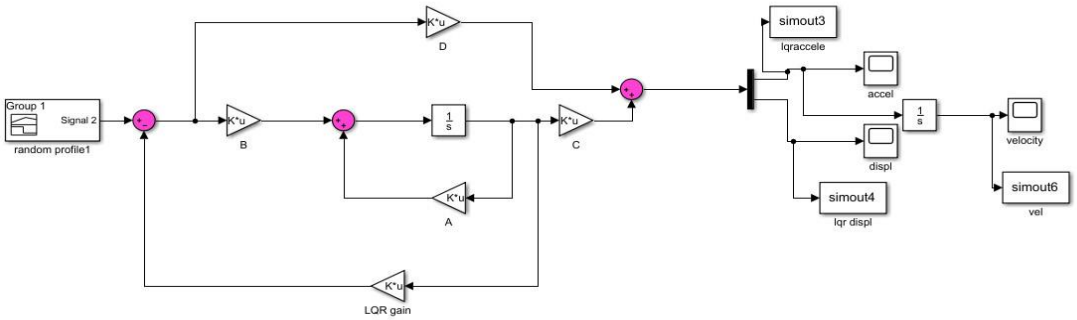

FIGURE 3. LOR control for the active seat test

The proposed controller technique's effectiveness, robustness, and power in terms of improving ride comfort were evaluated when the test rig model was subjected to road input. To generate road profile disturbance, two road types were used. The first was a bumpy road profile, based on equation (11) [20]:

$$y(t) = \begin{cases} (a\left(1 - \frac{\cos 8\pi t}{2}\right)) & 0.25 \le t \le 0.5 \\ 0 & otherwais \end{cases} \tag{11}$$

where (a) =10 is the bump height. The bumpy road profile is shown in fig. 4.

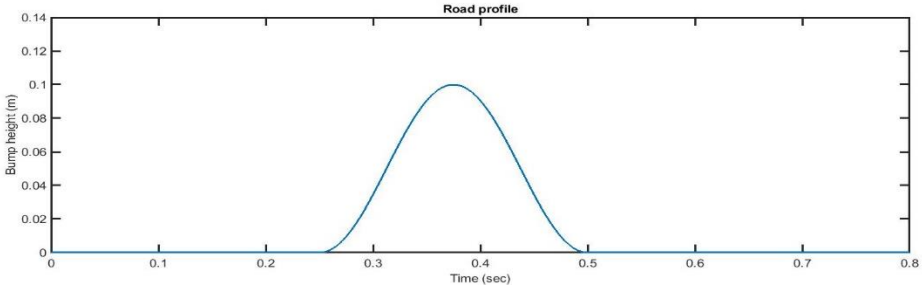

FIGURE 4. Bumpy road profile.

The simulation results for the bumpy road profile input showed an enhancement of response in the active system with LQR controller, based on the recorded values of R, as compared with the passive system; this applied across suspension travel, seat pan velocity, and acceleration. Two cases were determined, based on Q value:

a) Case one. The Q values were as follows:

$$Q = \begin{bmatrix} 13080.66706 & 2615.933413 & -13079.66706 & -2615.933413 \\ 2615.933413 & 523.1866825 & -2615.933413 & -523.1866825 \\ -13079.66706 & -2615.933413 & 13079.66706 & 2615.933413 \\ -2615.933413 & -523.1866825 & 2615.933413 & 523.1866825 \end{bmatrix}$$

One of the cost effects of using an LQR controller is that the amount of suspension travel will be increased. The designer can thus use this signal to find the limitations of the test rig system. From fig. 5, it is clear that the suspension travel increases relative to controller action and increased R:

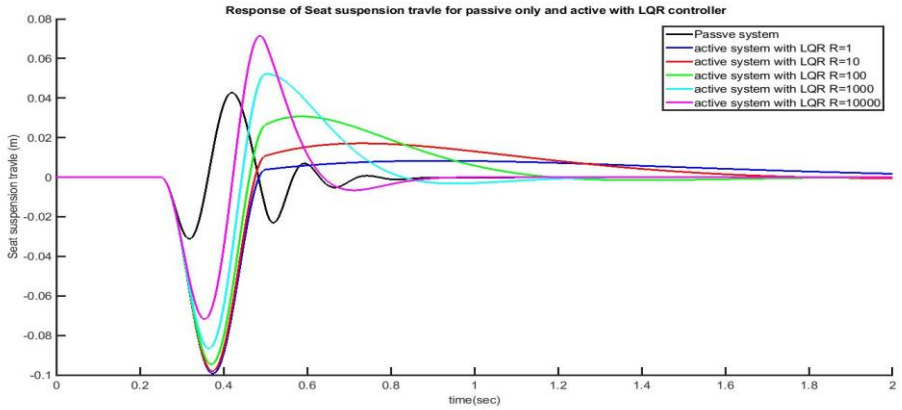

FIGURE 5. Seat suspension travel for the bumpy road profile.

Figures 6 and 7 show the behaviours of the seat pan velocity and acceleration for different R values in comparison with the passive responses for those values. The reduction in velocity was 98% for R=1, though the ratio decreased with increases in R-value to 53% at R=10,000. Similarly, for acceleration, at R=1, the percentage of reduction was about 98%, and this decreased with increases in R to 70%. It is thus clear that a reduction in both velocity and acceleration is seen based on controller action with different R values.

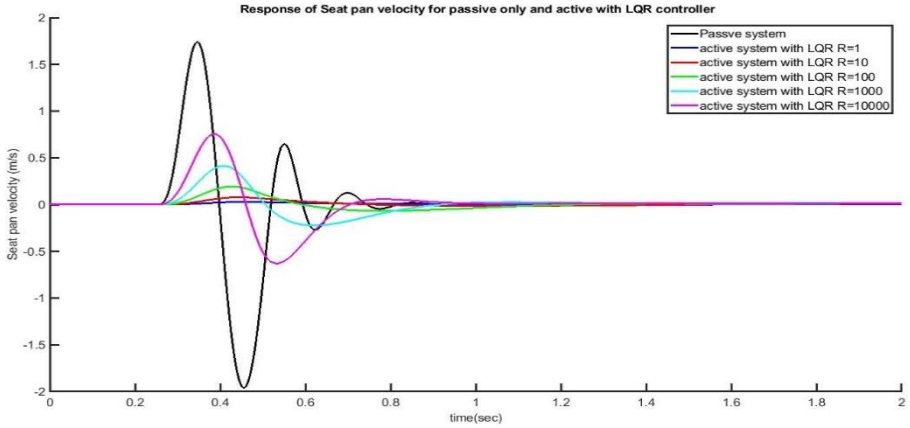

FIGURE 6. Seat pan velocity for a bumpy road profile.

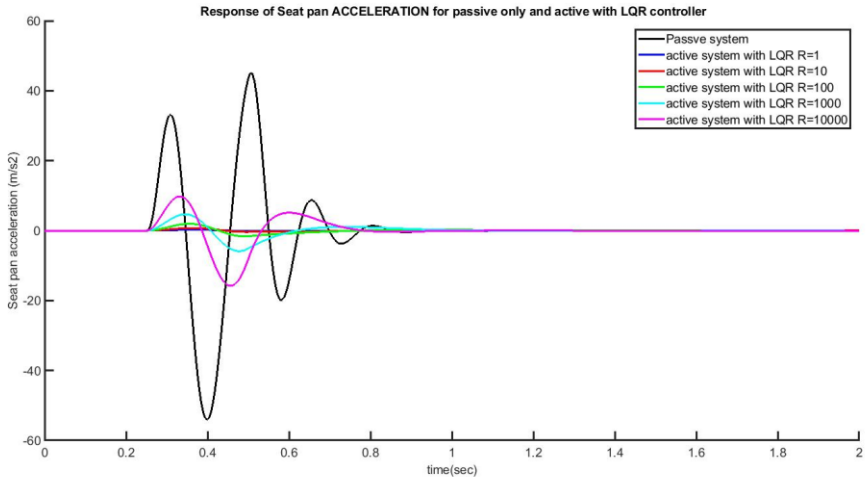

FIGURE 7. Seat pan acceleration for a bumpy road profile.

In addition, the results of using the first Q matrix with different values for R showed good improvement in the mechanical response performance and the stability of the seat pan in the active LQR system as compared to in the passive system. The LQR was more effective in reducing the velocity and acceleration of the seat pan, and, as a result, LQR successfully excluded many of the oscillations in signals to reach the steady-state more rapidly.

b) Case two. The Q values were as follows:

$$Q = \begin{bmatrix} 130.8066706 & 26.15933413 & -130.7966706 & -26.15933413 \\ 26.15933413 & 5.23.1866825 & -26.15933413 & -5.231866825 \\ -130.7966706 & -26.15933413 & 130.7966706 & 26.15933413 \\ -26.15933413 & -5.231866825 & 26.15933413 & 5.231866825 \end{bmatrix}$$

Based on this second set of Q values, a comparison of results for the active system using the LQR controller and the passive system relative to the bumpy profile input are shown in the following three figures for suspension travel, velocity, and acceleration, respectively.

As shown in fig.8, compared with the passive system, the LQR system increases suspension travel by 200% for a value of R=1, moving to 16% for a value of R=10,000.

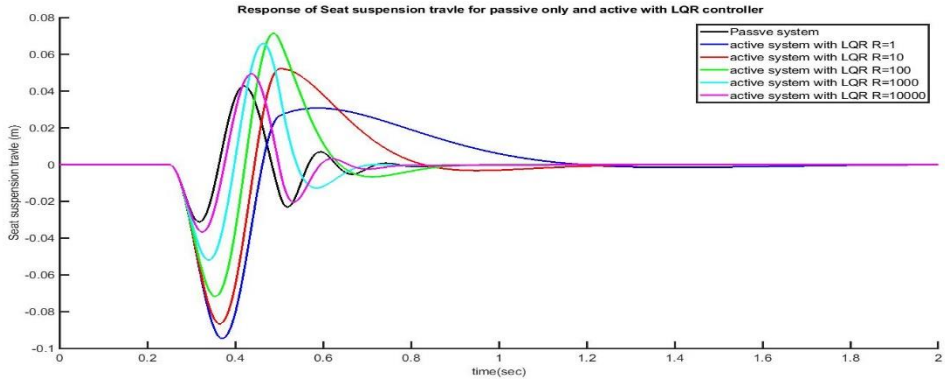

FIGURE 8. Seat suspension travel for a bumpy road profile.

Figures 9 and 10 offer a comparison between the passive system and the LQR controller system for different R values in terms of seat pan velocity and acceleration. A big reduction in velocity can be seen: for R=1, the decrease in velocity is about 88%, with a percentage change to 11% at R=10,000. There is also a good move within the acceleration to reduce the vibration, with it decreasing from about 94% at R=1 to 22% for R=10,000.

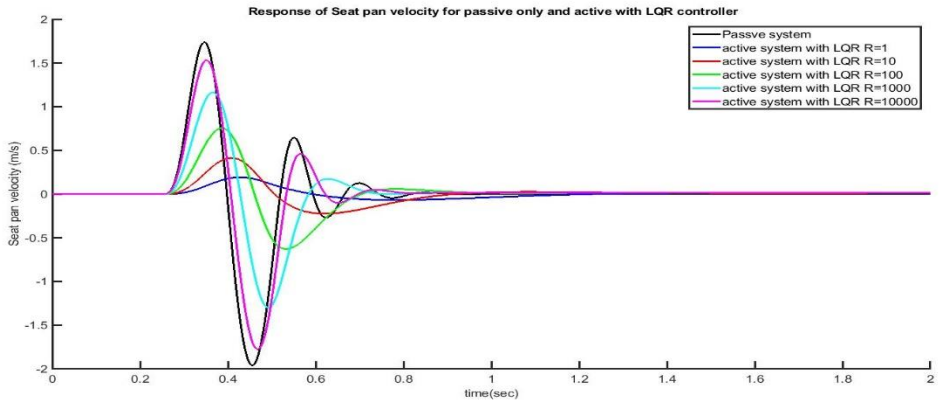

FIGURE 9. Seat pan velocity for a bumpy road profile.

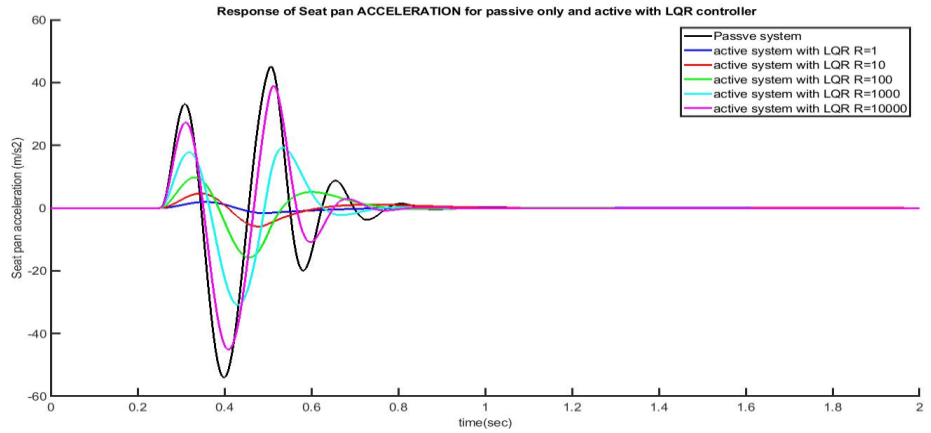

FIGURE 10. Seat pan acceleration for a bumpy road profile.

In general, using the second Q matrix shows that the LQR controller offers significant superiority over the passive system in terms of vibration reduction. Both Q matrixes provide good performance results, though there is some difference between them in terms of the second Q matrix clearly deriving the settling time to be shorter, thus reducing the overshot compared with the results seen for the first Q matrix.

The second road profile disturbance was a random road with road roughness $3\,m^3$, making it a class C according to ISO 8606; a vehicle speed of $20\ \mathrm{Km/h}$, was then set. Figure 11 shows the random road profile.

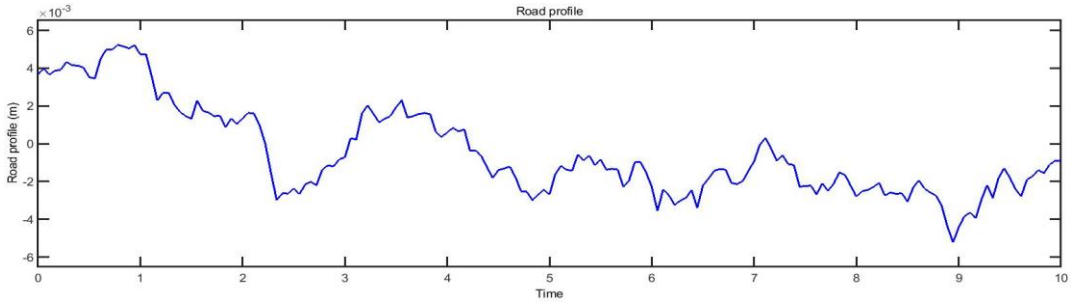

FIGURE 11. Random road profile**.**

A clear opinion on the system's behaviours within the employed LQR controller was found by combining two different Q matrix values with multi-value R.

a) Case one. The Q values were as follows:

$$Q = \begin{bmatrix} 13080.66706 & 2615.933413 & -13079.66706 & -2615.933413 \\ 2615.933413 & 523.1866825 & -2615.933413 & -523.1866825 \\ -13079.66706 & -2615.933413 & 13079.66706 & 2615.933413 \\ -2615.933413 & -523.1866825 & 2615.933413 & 523.1866825 \end{bmatrix}$$

Figure 12 shows the suspension travel for the random profile: here, the suspension travel increases relative to LQR controller action and increased R-value.

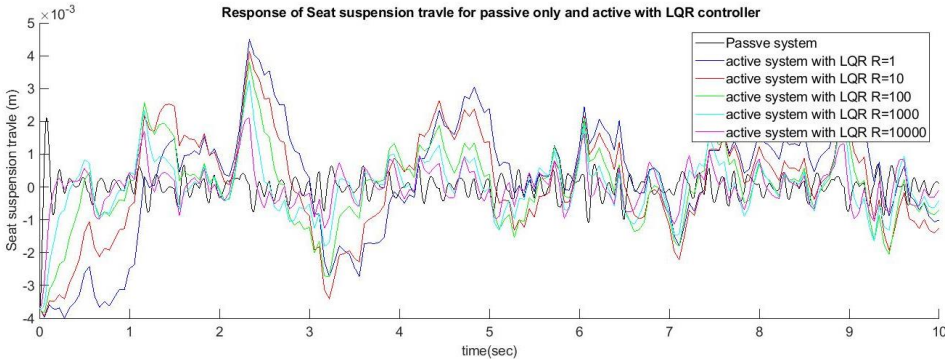

FIGURE 12. Seat suspension travel for random road profile.

Figures 13 and 14 show the seat pan velocity and acceleration responses for different R values as compared with the passive response according to the random disturbance road input. Clearly, the reduction in both velocity and acceleration is relative to a controller action within scope of the varying values of R.

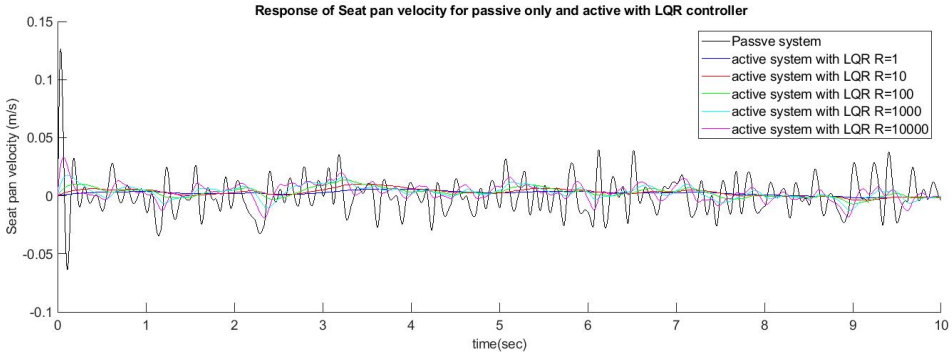

FIGURE 13. Seat pan velocity for random road profile.

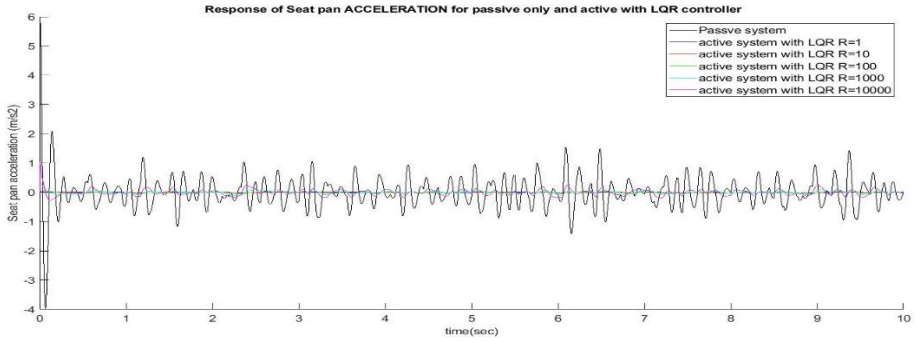

FIGURE 14. Seat pan acceleration for random road profile.

b) Case two. The Q value were as follows:

$$Q = \begin{bmatrix} 130.8066706 & 26.15933413 & -130.7966706 & -26.15933413 \\ 26.15933413 & 5.23.1866825 & -26.15933413 & -5.231866825 \\ -130.7966706 & -26.15933413 & 130.7966706 & 26.15933413 \\ -26.15933413 & -5.231866825 & 26.15933413 & 5.231866825 \end{bmatrix}$$

The following three Figures show a comparison of behaviour results between passive and active systems, based on considering the LQR controller relative to the random profile input in terms of suspension travel, velocity, and acceleration, according to the second Q value. In fig. 15, the control action on the suspension travel can be seen as increasing with decreasing R-values.

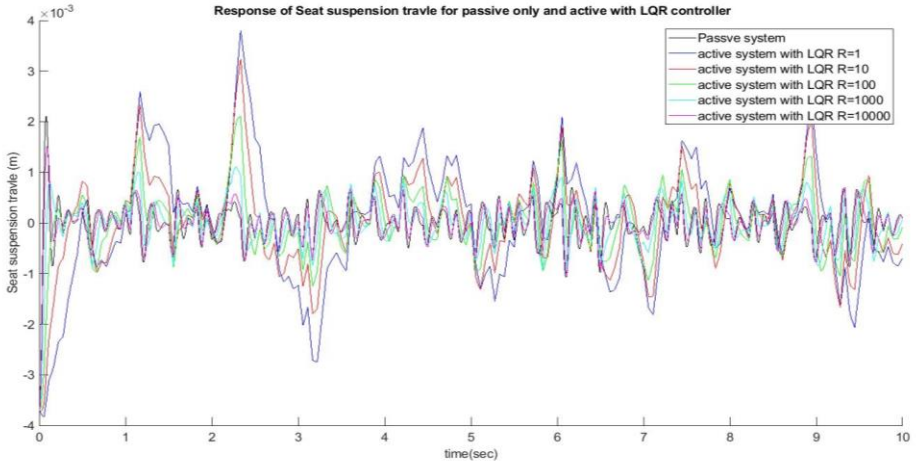

FIGURE 15. Seat suspension travel for random road profile.

Figures 16 and 17 show good performance for the LQR controller system in terms of reducing velocity and acceleration.

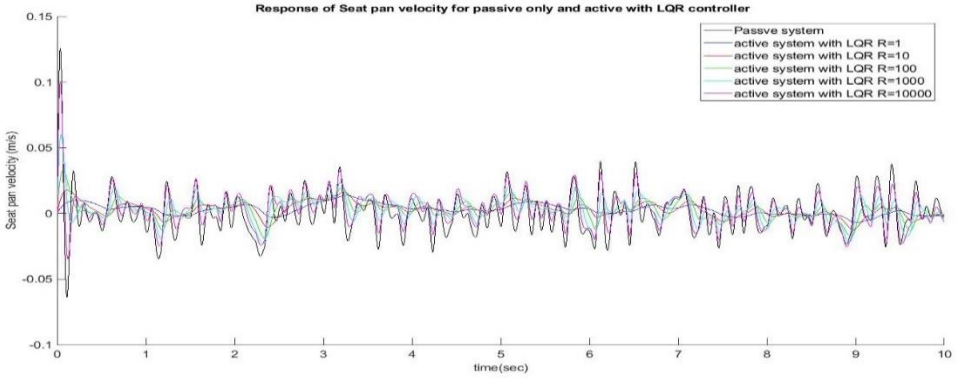

FIGURE 16. Seat pan velocity for random road profile.

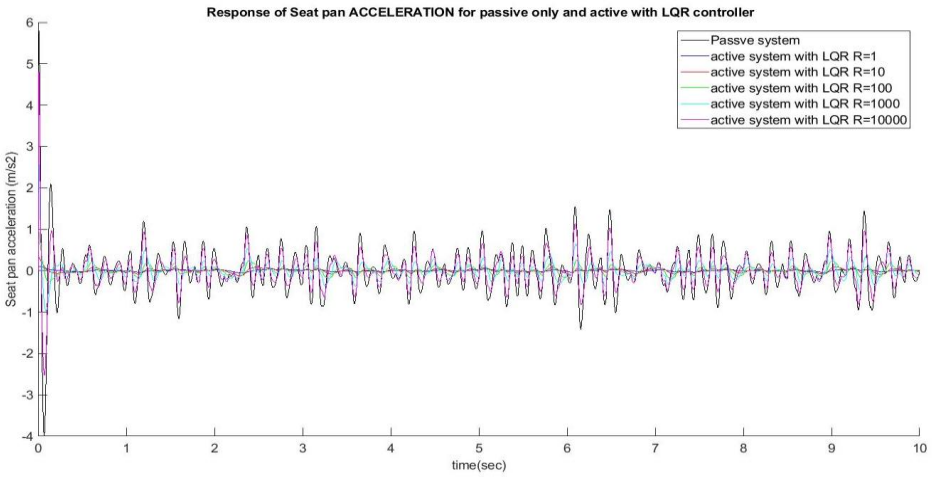

FIGURE 17. Seat pan acceleration for random road profile.

The results show good responses for the LQR controller in comparison with the passive system. It is also clear that the use of the second Q matrix case gives good performance in terms of settling time and reduction of overshoot percentage output.

In summary, using a linear quadratic regulator controller with the seat driver's test rig by identifying optimal values of R and Q provides good improvement in terms of seat ride comfort and clearly reduces vibration as compared with the passive system. The linear quadratic regulator controller has the ability to determine the best performance response in terms of the percentage of overshoot and the settling time in seat drive responses, based on reducing the velocity and acceleration of seat pan as determined by the optimal values for R or Q. This is achieved in the second case when the settling time changes by 38% and rise time reaches 81%, with a percentage overshoot of about 7%. The velocity decreases between 11 to 88%, with acceleration reduction of approximately 22 to 94%. Thus, in comparison to passive seat suspension, the active seat system with the LQR controller technique achieves lower amplitudes and faster responses in the case of seat pan suspension deflections and acceleration.

6. CONCLUSION

In this paper, the verification of a simulation design using a linear quadratic regulator control technique was used to successfully drive a seat drive's system test. Performance enhancement was achieved by the response of the seat test rig system, while the linear quadratic regulator controller was examined in conjunction with two different road profiles, a random and a bumpy road profile, to extend the scope of input control and state matrix values. The controller action demonstrated good robustness as well as being realisable. The optimal linear quadratic regulator controller stabilised the seat system more effectively in comparison with the passive system. Based on the results, the passive system as combined with an optimal linear quadratic regulator controller design achieved the best ride comfort performance, significantly reducing seat pan acceleration by about 90%.

ACKNOWLEDGMENTS

The authors would thank Kerbala University, Engineering College for the opportunity to do this study. They would also like to thank Al-Furat Al-Awsat Technical University/Technical Institute of Al-Mussaib/Mechanic department, Dr Kamil J. Kadhim, Dr Zaid H. Rashid, and the laboratory technician "Laith Abdul Rahim" for their support.

REFERENCES

1. Gan, Z, Hillis, A and Darling, J, Journal of Sound and Vibration **349**, 39-55 (2015).
2. Alfadhli, A., Darling, J. and Hillis, A.J., Applied Sciences **8**, 603(2018).
3. Zhao, Y. and Wang, X., Applied Sciences **9**, 3326(2019).
4. Alfadhli, A., Darling, J. and Hillis, A.J., Vibration **1**, 20-40(2018).
5. Al-Ashmori, M. and Wang, X., Applied Sciences **10**, 1148(2020).
6. Appleyard, M. and Wellstead, P.E., IEE Proceedings-Control Theory and Applications **142**, 123-128(1995).
7. Sun, S., Ning, D., Yang, J., Du, H., Zhang, S. and Li, W., IOP Science, Smart Materials and Structure **25**, 105032(2016).
8. Wu, X. and Griffin, M., Journal of Sound and Vibration **203**, 781-793(1997).
9. Hussein, Emad, The Iraqi Journal For Mechanical And Material Engineering **14**, (2014).
10. Al-Zughaibi, A., Xue, Y., Grosvenor, R. and Okon, A., Journal of Automobile Engineering, **233**, (2019).
11. Hussein, E., Al-Dujaili, A. and Ajel, A., IOP Conference Series: Materials Science and Engineering **881**, 012084(2020)
12. Ali I. Al-Zughaibi1, Emad Q. Hussein and Noor Abbas, Design Engineering (Toronto) **2021**, 6644-6655(2021).
13. R. Darus and N. I. Enzai, International conference on Science and Social Research (CSSR), Kuala Lumpur, Malaysia (IEEE, 2010), pp.1203-1206.
14. Sam, Y. M., Ghani, M. R. A. and Ahmad, N., International Conference on 2000 TENCON Proceedings. Intelligent Systems and Technologies for the New Millennium **1**, (IEEE, 2000), pp. 441-444.
15. Borozan, I., Cosco, F. and Argesanu, V., Applied Mechanics and Materials **811**, 199-203(2015).
16. Maurya, V. and Bhangal, N., Journal of Automation and Control Engineering **6**, 22-26(2018).
17. Okyere, E., Bousbaine, A., Poyi, G. T., Joseph, A. K., and Andrade, J. M., the 9th International Conference on Power Electronics, Machines and Drives,(The Arena and Convention Centre, Liverpool, London: The Institute of Engineering and Technology, 2018), pp.1-7.
18. Sushamshushekar Doddabasappa, "LQR control design for a dc-dc converter using sensitivity functions". Master thesis, The Pennsylvania State University the Graduate School, 2019.
19. Nagarkar, M. P. and Patil G. J. V., 2012 Third International Conference on Computing, Communication and Networking Technologies ICCCNT'12, Coimbatore, India (IEEE, 2012).
20. I. J. Fialho and G. J. Balas., Vehicle System Dynamics **33**, 351–370(2000).